ACTA IMEKO
ISSN: 2221-870X
December 2023, Volume 12, Number 4, 1 - 8

Acquisition and integration of differential pressure measurements on sails for boat performances improvement

Antonio Affanni[1], Luca Casarsa[1], Ivan Scagnetto[2], Francesco Trevisan[1]

[1] *Polytechnic Department of Engineering and Architecture DPIA, University of Udine, Via delle Scienze 206, 33100 Udine, Italy*
[2] *Dipartimento di Scienze Matematiche, Informatiche e Fisiche DMIF, University of Udine, Via delle Scienze 206, 33100 Udine, Italy*

ABSTRACT
In this paper, we integrated within a specifically developed acquisition system, denoted as Oceanus, the measurements from a differential pressure sensor between the two sides of a sail (windward and leeward sides); experiments have been performed using a light jib sail of a 35 feet cruising-racing yacht. We analyzed the correlation between such a signal and other standard signals usually present on board such as boat speed, intensity and direction of apparent or real wind; moreover, data from Inertial Measurement Units are handled. We also considered the Target Data, which depend on the actual point of sail, and the discrepancy between measured data and the predicted Targets is monitored as an error in terms of the true wind angle and boat velocity. In this way, the trimmer/helmsman can monitor the differential sail pressure together with Target data and decide to reduce the error with a correction in how sails are trimmed, rather than in how the boat is steered to achieve an improvement of boat performances. The resulting telemetry system represents an effective low cost solution, which is affordable even for amateur yachtsmen.

Section: RESEARCH PAPER

Keywords: Target data; GPS data; wind measurements; sail differential pressure

Citation: Antonio Affanni, Luca Casarsa, Ivan Scagnetto, Francesco Trevisan, Acquisition and integration of differential pressure measurements on sails for boat performances improvement, Acta IMEKO, vol. 12, no. 4, article 6, December 2023, identifier: IMEKO-ACTA-12 (2023)-04-06

Section Editor: Laura Fabbiano, Politecnico di Bari, Italy

Received April 18, 2023; **In final form** November 7, 2023; **Published** December 2023

Corresponding author: Antonio Affanni, e-mail: antonio.affanni@uniud.it

1. INTRODUCTION

Both racing and cruising yachts, even for amateur, have become more and more demanding in terms of boat performances; as an example, most of the crew members use polar diagrams of the boat to compare in real time the actual boat speed and angle to the wind, with respect to the optimal speed and angle that the boat is capable of in the actual wind conditions. Such optimal data, often referred to as Target Data are the result of a numerical simulation performed by means of the Velocity Prediction Program (VPP) released by the Offshore Racing Congress [1] on the bases of the actual geometry of the boat hull, of the sails dimensions and of the dynamic boat behaviour.

However, the direct results from the VPP might not be accurate enough due to the complexity of the physics behind and the unavailability of detailed sail performance data. Therefore, racing teams develop their own ad-hoc software to compute target data, which is successively fine-tuned by means of dedicated sea trials. Another approach could be to look at real-time sail performance data and link them to the actual boat course and speed to adjust sail trim and boat steering towards the optimal set, to achieve performances that go beyond the level that the average crew can reach based only on experience. To this aim, sail pressure distribution can be a candidate to look at.

Few contributions are available in literature about pressure distributions on upwind sails and an example can be found in [2]. They performed pressure measurements on several horizontal sections of a head and main sail, both on leeward and windward sides, providing information about sail aerodynamic (e.g., the laminar to turbulent transition, the leading-edge separation and reattachment, and the trailing edge separation) and partial indication useful for sail trimming. Upwind sail differential pressure measurement system has been also developed by [3], [4], validated on a wind tunnel model and successively tested in full scale. Their measurement system is based on expensive MEMS sensors that receive the signal from pressure strips and pads sewed on the sail. Therefore, it is a system that is more likely to be used for research purposes on sail aerodynamics rather than on the field. Pressure measurements have been used for research on spinnaker aerodynamics also in [5]-[8], and coupled with sail

shape measurements to get significant insight about downwind sail aerodynamics. However, the large array of sensors they employed is physically connected by wires that run on sail skin and luff, making the installation also in this case not suited for long life, easy to handle service.

With the aim of performing full-scale measurements, in our Sailing Laboratory, according to the system integration logic, we designed a low cost, but reliable telemetry system, denoted as Oceanus [9], whose hardware can be easily scaled, in order to include different kinds of sensors and devices.

The developed integrated system is capable of acquiring, logging and processing data from a number of sensors or cluster of sensors within a proprietary network, by means of dedicated threads; in this way, different baud rates can be managed and integrity of data is assured in any condition.

In particular, the acquired data are wind amplitude and direction both with respect to the boat and referred to ground, Roll and Pitch from an Inertial Measurement Unit attached to the centre of mass of the boat. A GPS completes the set of standard data providing the time-base of the acquisition, the Course Over Ground and the Speed Over Ground.

We developed and characterized a sensor capable of measuring the differential pressure between the windward and the leeward part of the jib located in the middle of the 1/4 section of the jib luff; then, we integrated it into the Oceanus System. The sensor has been specifically designed to communicate wirelessly with the Oceanus System; in this way, complicated pressure taps and long tubes layouts, requiring a reference unperturbed static pressure measurement, can be avoided, [10]-[13].

For the experiments, we used an Archambault A35 cruising-racing yacht equipped with a main sail and a light jib rated for winds up to 13 kn.

We performed multiple upwind navigations under almost constant wind speed and angle for a sufficiently large time intervals resulting in an almost constant course; we acquired all data computing the data fusion between sensors, in order to verify the correlation with the differential pressure signal, gaining, in this way, information for helmsman and tailer. The helmsman can monitor the target data for the current point of sail, in order to react quickly, improving the boat performance as the wind conditions change.

The aim of this work is to present the designed wireless pressure sensor, to show its performances by means of its characterization in a wind tunnel and to provide its functionality during navigation. In particular, the tests in the sea were focused on performing a sensitivity analysis, to explore the extent of information from the differential pressure sensor and how such further signal is correlated with other available navigation signals.

The experiments showed how it was possible to correlate the single-point measurement pressure signal to other boat data. Therefore the system, although limited to a single point measurement, can be profitably used to improve sail trimming and boat performances. Even though sail aerodynamics is not the object of the present investigation, the system can be easily improved to a multipoint configuration by adding other sensors in significant locations to cope with fluid dynamics analysis.

In addition, an important novelty of our proposed contribution is that it has been achieved with very low costs both in terms of money (needed to buy and integrate the hardware and sensors) and in terms of simplicity and modularity of the on-board installation and configuration. Indeed, a Raspberry Pi 3B+ with a 32 GB sd-card, a Tinkerforge IMU Brick 2.0, a Kendau MG-220 GPS, a CMPS14 digital compass, a powerbank of 24 Ah, and the differential pressure sensor described in Section 2.3 cost under 350 EUR. Moreover, all the connections are very simple and the pressure data are communicated via the local Wi-Fi hotspot created by the Raspberry Pi. Hence, even an amateur yachtsman could easily repeat our experiments, with a limited expense and a few hours of work, to buy and install all the above mentioned equipment described in full details in the following Sections.

2. MATERIALS AND METHODS

Depending on the level of equipment on board, a dedicated bus connects different sensors transmitting data during each data production cycle; a typical installation consists of: a flux-gate compass for the Magnetic Heading (MH) of the aft-bow longitudinal axis with respect to the magnetic north, a speedometer sensing the Speed Over Water (SOW) component along the longitudinal boat axis, a wind station on the top of the mast, sensing the Apparent Wind Speed (AWS) and Apparent Wind Angle (AWA) with respect to the longitudinal boat axis. We will denote such quantities as primary quantities since they are directly measured by a dedicated sensor. From a subset of primary quantities, a number of secondary quantities are usually computed and are available on the bus together with the primary ones. As an example, from the triple SOW, AWS, AWA the so called True Wind Speed (TWS) sensed by an observer fixed with respect to the ground is computed; similarly for the corresponding True Wind Angle (TWA) with respect to the longitudinal boat axis. In addition, from the pair MH, TWA, the Magnetic Wind Direction (MWD) is computed with respect to the magnetic North. Such installation represents a closed hardware and software infrastructure; thus, the input/output interaction with other devices or sensors is provided by a dedicated input/output interface, which allows the bidirectional conversion of the data present on proprietary bus to a public data bus. Usually, a NMEA 0183 interface allows the conversion of data present on the proprietary bus onto the data bus, so as to allow the interfacing between the proprietary network of devices and external devices from a different manufacturer. A typical external device, interfaced with the closed hardware and software infrastructure, is a GPS; it provides as output in NMEA 0183 format at least the latitude, longitude, Speed Over Ground (SOG), Course Over Ground (COG), time and date; in the case of a cartographic GPS, way points setting and the corresponding cross track distance and course are sent in addition.

The rationale of the Oceanus project is to set up an independent acquisition unit, with in house developed software, capable to record and process primary and secondary quantities generated not only from the existent closed infrastructure but also from a number of different independent devices. To this purpose, we used an RS232 serial port to interface the closed infrastructure to a Raspberry Pi 3 computer. We interfaced a further GPS unit, an Inertial Measurement Unit (IMU) and the Differential Sail Pressure Unit (DSPU) described in detail in Section 2.3.

2.1. Oceanus hardware and software architecture

In order to contain power consumption, while retaining the capability to customize the system by adding new devices and sensors, and changing code and settings on the fly, we implemented the prototype version of our on-board telemetry system using a Raspberry Pi 3 (model B+) device and peripherals commonly available on the market. The power supply is a power

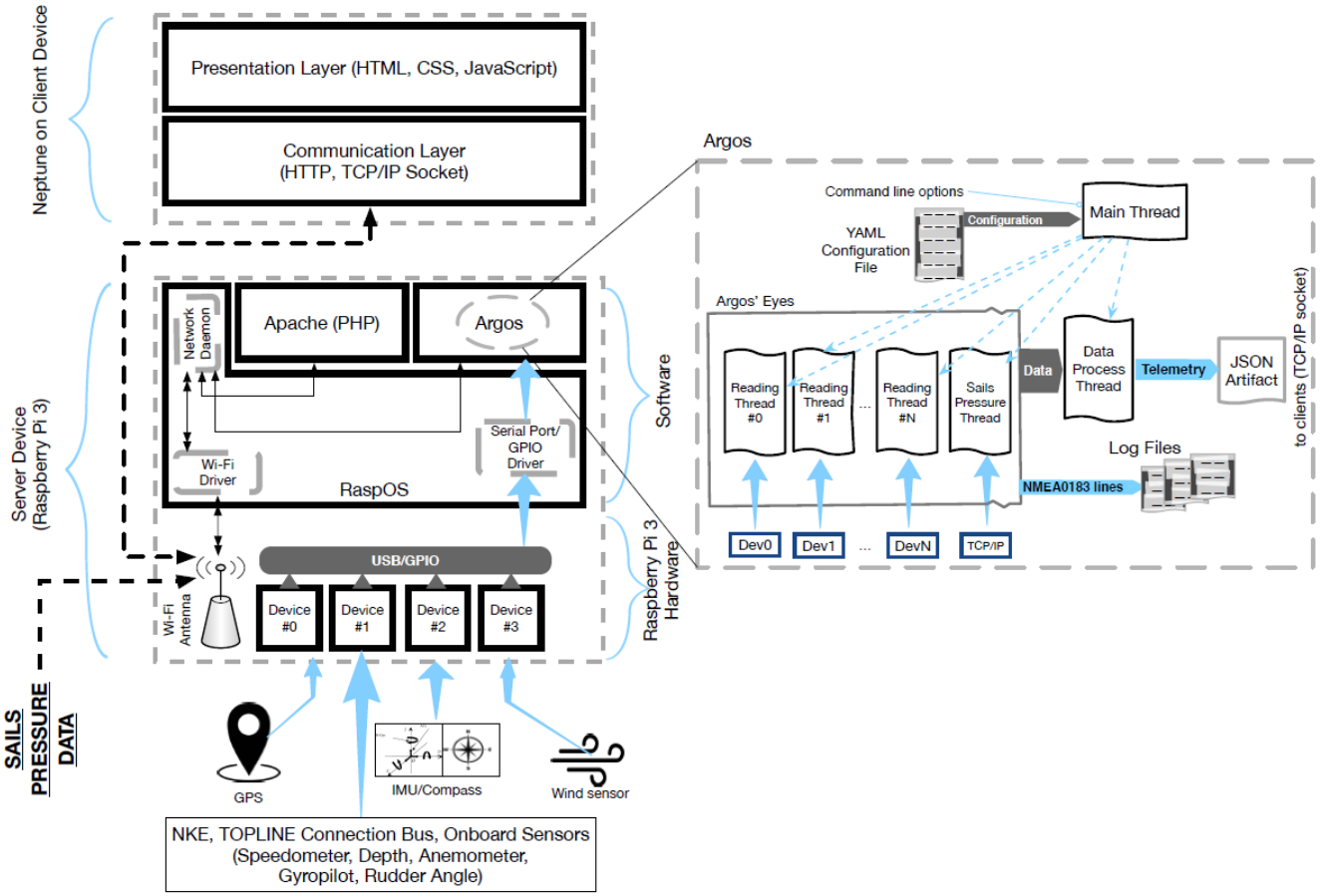

Figure 1. Hardware and software architecture of the telemetry system.

bank of 24 Ah, which, according to our tests, allows the system to stay up for 9 hours. The Raspberry Pi allows us to:

i. harvest raw data from sensors (connected through USB ports, a Wi-Fi connection and the I²C bus);
ii. compute meaningful and useful information from raw data;
iii. provide a Wi-Fi local area network (WLAN);
iv. publish the computed information through a socket service and a web application in the WLAN;

In this way, human operators on-board can easily monitor and control the data flow provided by the Raspberry Pi device, using their smartphones, tablets etc. (via the above mentioned web application).

Figure 1 illustrates the details and the interactions of the hardware and software components used in our architecture. The core element is the Raspberry Pi computer, which is physically connected to the remaining devices through its USB ports, the GPIO interface and the WLAN. A serial connection to the on-board electronic bus (in our specific case, a NKE bus) collects the main data measured on-board like, e.g., apparent and real wind amplitude and angle, depth, course, speed over ground, latitude and longitude, magnetic heading, velocity with respect to water, etc. The other devices we usually connect to the USB ports are a GPS receiver (used also as time base), an ultrasonic wind sensor, and an IMU device. Finally, the connection with the differential pressure measurement on the sail DSPU is implemented through Wi-Fi socket connections.

From the software point of view, the core element is the Argos [9] server component, which runs on the Raspberry Pi (see Figure 1), being entirely written in C language. Its purpose is to interface the sensors through the drivers of the underlying operating system of the Raspberry Pi (RaspOS), reading data from USB ports and the GPIO pins. Both the GPS receiver and the wind sensor release a stream of NMEA 0183 sentences over a serial communication interface. The IMU sends its data through the USB bus as well. Instead, as we mentioned before, the direction w.r.t. the magnetic north is acquired from a CMPS14 digital compass connected to the Raspberry Pi via its GPIO pins. Hence, the angle data can be read via the I2C bus; then, Argos adds such angle to the angle provided by the wind sensor, to calculate the direction of the wind w.r.t. the magnetic north. Sails pressures are received via the local WLAN provided by the Raspberry Pi computer. Indeed, Argos listens on a TCP socket (by default the port number is 8899, but it can be easily changed via a YAML-formatted configuration file) incoming connections from the sensors mounted on the sails.

In order to cope with the different communication rates of the sensors, a separate thread is started for the GPS receiver, the wind sensor, the digital compass, and the sails pressures readings. So doing, the data harvesting is not hindered by slow sensors and no data are lost.

Moreover, thanks to this kind of multithreading, there is always a representation of the current values of all sensors stored in the memory of the Raspberry Pi device. This allows us to send

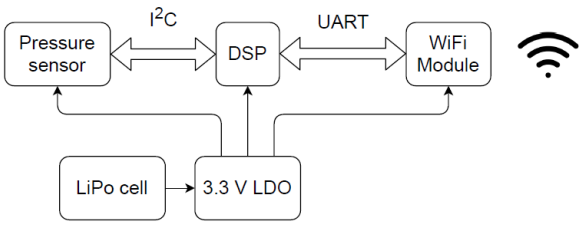

Figure 2. Wireless pressure sensor block diagram.

such information on demand to the web application (Neptune) at regular intervals.

Finally, all the activity is logged permanently on the local filesystem of the Raspberry Pi device by another ad-hoc thread (at intervals of 30 s).

The crew can visualize all the relevant information computed by Argos by means of the Neptune web application [9], which can be accessed by any device with a JavaScript-enabled browser and a Wi-Fi network card (see the top part of Figure 1).

2.2. Inertial Measurement Unit

The Inertial Measurement Unit (IMU) is equipped with a 3-axis accelerometer, magnetometer (yielding a three axes compass) and gyroscope and interfaces with Oceanus by means of a USB port. It can measure 9 degrees of freedom and computes Quaternions, Linear Acceleration, Gravity Vector as well as independent Heading, Roll and Pitch angles. It is a complete attitude and heading reference system.

2.3. Differential Sail Pressure Unit

The block diagram of the developed wireless Differential Sail Pressure Unit is shown in Figure 2.

The power supply is provided by a single cell Lithium Polymer (LiPo) battery whose capacity is 850 mAh; the voltage is regulated by a low dropout (LDO) voltage regulator which provides 3.3 V supply for the entire circuitry. The sensing element is the Sensirion SDP810-125Pa, whose input range is ±125 Pa and the output is provided with Inter-Integrated-Circuit (I²C) serial protocol; the sensor provides 16-bit wide pressure data, corresponding to a resolution of 3.8 mPa [14]. A DSP (DSPIC30F3013 from Microchip) communicates with the sensing element and acquires the pressure data by sending I²C queries every 100 ms corresponding to the sampling rate f_s = 10 Hz. The acquired pressure data are then sent to a low power Wi-Fi module using Universal Asynchronous Receiver/Transmitter (UART) protocol. The Wi-Fi module (USR-C216 from USR-IOT) is wirelessly connected to the access point on the boat and transmits the data to the server through TCP/IP protocol.

Figure 3. PCB realization of the wireless pressure sensor mounted on the sail.

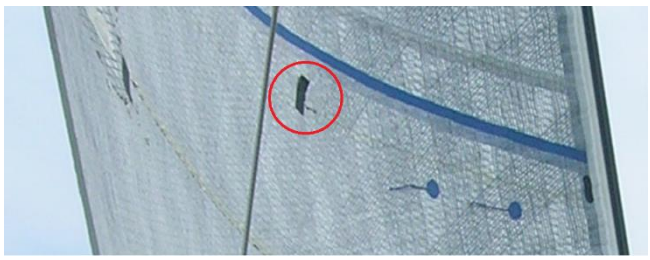

Figure 4. Detail of the jib at maximum trim where the windward straight tell-tails are shown; moreover, the differential sail pressure unit is evidenced within the circle.

The current consumption of the wireless sensor is 80 mA during transmission; thus, the battery capacity assures more than ten hours of continuous operation. The sensor has been realized on a 2-layers PCB whose dimensions are 30×56 mm².

The sensor board is mounted on the jib sail by means of sail adhesive tape, as shown in Figure 3; the pressure inlets are taken by posing two short tubes at the two sides of the sail and oriented perpendicularly with respect to the wind direction (in particular the tubes inlets are oriented to the top).

3. EXPERIMENTAL RESULTS

3.1. Measurement setup

We installed on a light jib of 29 m² the differential pressure unit in proximity to the tell-tails attached to the sail, used as a guide for trimming (adjusting) a sail, Figure 4. On the jib, there are tell-tails on both sides of the luff of the sail; as a general guide, during upwind navigation, the windward-leeward tell-tail should stream aft (backwards) and parallel each other with an occasional lift. We started an upwind navigation both on port and starboard side under almost uniform wind direction with respect to the north and TWS in the range between 10 kn to 13 kn.

The jib has been set at the so called maximum trim condition in order to provide the minimum TWA (around 40 DEG) at the maximum speed over ground (around 6.2 kn) compatible with the boat in this wind conditions; the AWA was around 30 DEG yielding the angle of attack of the jib even though measured on the top of the mast. To reach and monitor such starting condition, we used both the visual information from tell-tails and the real time data provided by the developed web interface showing the discrepancy with respect to the simulated Target Data.

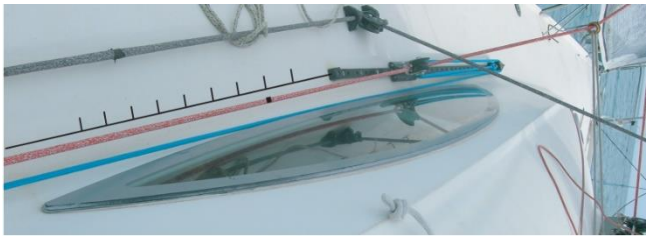

Figure 5. A ruler parallel to the jib sheet measures, with respect to a reference mark drawn on the sheet, the extent of loosing of the sail from the position of maximum trim. The jib carriage is kept fixed during the measurement procedure.

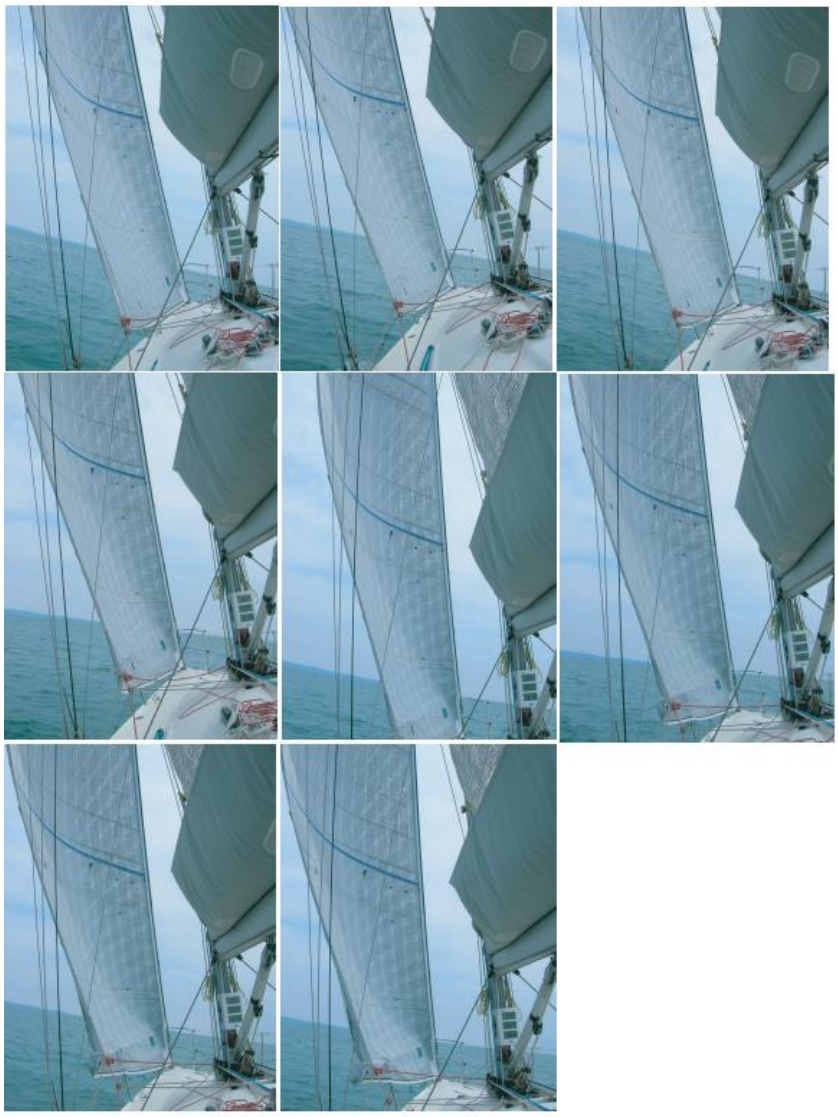

Figure 6. Geometry of the jib form the full trim position (top left image) to the completely loosen position (bottom right image).

In this way, the course was almost constant for a sufficient large time interval during which the measurement data was acquired. The main sail regulation was kept constant.

Next, starting from the maximum trim condition, we loose in steps of 5 cm the jib sheet used to control the shape of the sail. The constant course was guaranteed by the autopilot locked at the reference Magnetic Heading. We used a ruler drawn parallel to the jib sheet to measure the extent of the steps of loosing of the sail from its initial position of maximum trim, Figure 5; the jib carriage position was kept constant. In Figure 6 the geometry of the jib is shown starting from the maximum trim configuration to the final completely loose jib configuration.

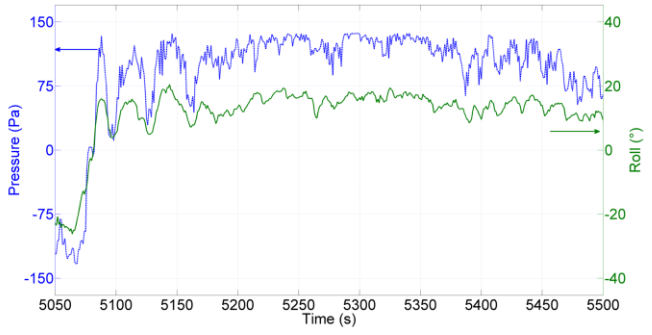

Figure 7. Differential Pressure on the jib correlated with the Roll angle of the boat both on starboard and port sides respectively.

3.1.1. Signal processing

In order to characterize the jib efficiency during sea manoeuvres, as it will be shown in Section 3.3, we needed to post process the pressure raw data acquired during the navigation. In particular, pressure data are affected by the roll angle of the boat due to the wind action on the sails, which causes a natural oscillation of the mast.

Figure 7 shows the differential pressure (blue line) acting on the jib and the roll angle (green line) of the boat during a tack and in straight sailing; the tack is shown in the initial part of the diagram where the differential pressure changes from below - 100 Pa to above 100 Pa.

The trend of the two quantities appears strongly correlated, at every Roll oscillation of the boat corresponds a change in Differential Pressure on the jib.

The correlation coefficient η between these quantities results $\eta = 96$ %.

In order to remove the effects of this correlation, which yields to artefacts in pressure readings, we applied a zero-phase forward and reverse digital low-pass filtering, with cut-off frequency 0.01 Hz.

3.2. Sensor Characterization

The pressure transducer and associated measurement chain described in Section 2.3 were experimentally characterized in terms of linearity response.

For this purpose, the transducer ports were connected to an aerodynamic probe, namely to the total and static pressure ports of a Pitot tube (as shown in Figure 8). The probe was then installed at the outlet of an open loop wind tunnel where the flow speed could be varied by acting on the inverter driving the wind tunnel fan (Figure 9). In this way, it was possible to impose the desired pressure difference at the

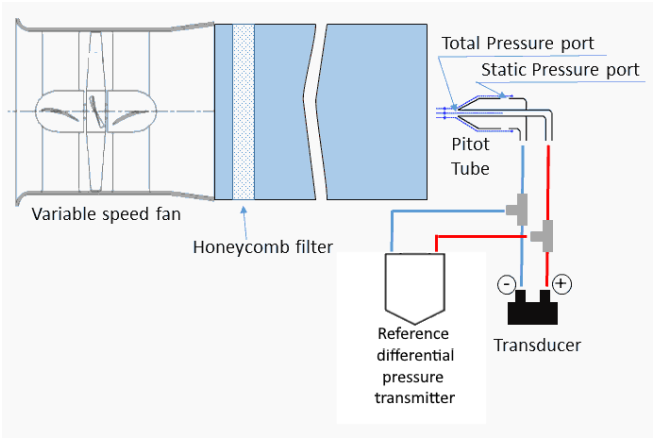

Figure 8. Experimental set-up for linearity error determination.

transducer (i.e. the flow dynamic pressure, the difference between the total and static one) within its actual range (± 125 Pa). Downstream of the wind tunnel fan, honeycomb flow straighteners were used to suppress flow swirl induced by the fan impeller and to smooth down flow turbulence to few percent of the bulk velocity. In order to test the device with positive or negative input signals, experiments were repeated by switching the connections of the transducer to the probe. A high accuracy differential pressure transmitter (Yokogawa EJX110A) was connected in parallel to the transducer and used as reference value for linearity checking. The readings expanded uncertainty due to the reference sensor is, accordingly to the instrument manual, 0.04 % of Span (considering the Span set to 500 Pa) thus resulting $u_B(P_S)$ = 0.06 Pa, a value below the expected linearity error of the device under test. Figure 9 shows the wind tunnel with Pitot tube, the reference sensor and the system under test used during the characterization.

In order to characterize the linearity of the wireless pressure sensor, we acquired the transmitted data varying the fan speed. The wind pressure was varied in the range [−120, 120] Pa, which we spanned in M = 23 steps; at the same time, for each step we measured the reference pressure from the transmitter. At each pressure step i we acquired N = 300 pressure samples $P_{S,ij}$ at a sampling frequency of 10 Hz (i.e. 30 s of acquisition for each pressure step). We selected this sample size by verifying that the acquired data exhibited a flat spectrum, as Gaussian white noise. This step assured the absence of any deterministic turbulence-related influences during the measurements. Additionally, the remarkably low turbulent content of the wind tunnel (approximately 3 %) played a crucial role in achieving this. Thus, the choice N = 300 ensures the collection of a significant set of uncorrelated samples, in order to perform type A estimation of the uncertainty according to the Guide to the Expression of Uncertainty in Measurement (GUM) [15]

$$u_A(P_{S,i}) = \sqrt{\frac{1}{N(N-1)}\sum_{j=1}^{N}\left(P_{S,ij} - \overline{P_{S,i}}\right)^2}. \quad (1)$$

From the 23 × 300 matrix of pressure acquisitions, we obtained the mean value of each step and its combined uncertainty. The combined uncertainty on pressure readings thus results from

$$u_C(P_{S,i}) = \sqrt{u_A^2(P_{S,i}) + u_B^2(P_S)}. \quad (2)$$

In order to perform linearity analysis, we used the least squares method using the reference pressure measurements from the transmitter $P_{REF,i}$ and the computed sample means $P_{S,i}$. The resulting gain G thus is

$$G = \frac{\langle P_{REF} \odot \overline{P_S} \rangle - \langle P_{REF} \rangle \langle P_S \rangle}{\langle P_{REF} \odot P_{REF} \rangle - \langle P_{REF} \rangle^2}, \quad (3)$$

where ⊙ indicates the Hadamard product.

Recalling that the vector P_{REF} is composed of M = 23 test pressures and that the vector P_S is obtained calculating the mean of 300 readings for each input pressure, the estimation of the gain uncertainty can be computed as:

$$u(G) = \sqrt{\sum_{i=1}^{M}\left(\frac{\partial G}{\partial P_{S,i}} u_C(P_{S,i})\right)^2}. \quad (4)$$

Using the gain calculated in Equation (3) and Equation (4), which numerically resulted into G = 1.0341 ± 0.00024, we evaluated the deviation from linear regression. In Figure 10, we show the linearity error expressed in pascal, where error bars represent the uncertainty calculated as described in Equation (2).

From Figure 10 it is possible to see that the maximum non-linearity of the wireless pressure sensor is ≈ 0.4 Pa with maximum uncertainty ≈ 0.08 Pa.

3.3. Results during sea manoeuvres

As discussed in Section 3.1, measurements were acquired both during tacks at an almost constant AWA and at different jib trims, i.e., at different length of its sheet measured with respect to a reference ruler, as shown in Figure 5. Figure 11 shows the averaged values of AWS and AWA measured during the tests. Thanks to effective setting of the boat autopilot, the AWA was kept constant at about 29 ° with a variability of ± 1 ° on both sides; however, wind and sea conditions slightly changed during the tests. On the starboard tack, the averaged wind speed was about 16.5 kn, with variations of ± 4 %. On the port tack, the average speed was lower and continuously decreasing during the session with averaged values from 15 to about 14 kn. Consequently, the boat Speed Over Water SOW was also different, with higher values in the condition of more wind, as it can be observed in the plot of Figure 12.

The differential pressure ΔP developed on the two surfaces of the sail is proportional to the square of the Apparent Wind Speed AWS and inversely proportional to the density of air ρ, accordingly to

$$\Delta P = C\,\rho\,S\,\frac{AWS^2}{2} \quad (5)$$

where S is the sail area and C is a global coefficient accounting for different contributions to the lift of the sail (mainly sail shape

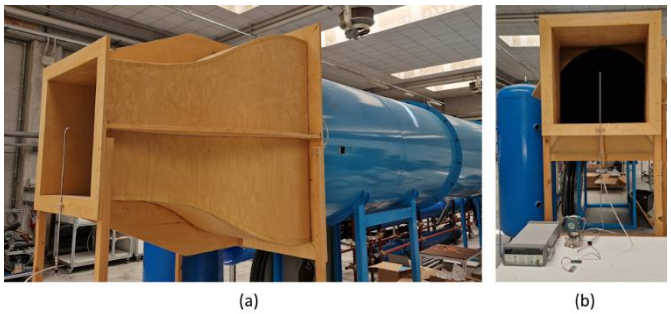

Figure 9. (a) wind tunnel with Pitot tube, (b) Reference sensor and system under test.

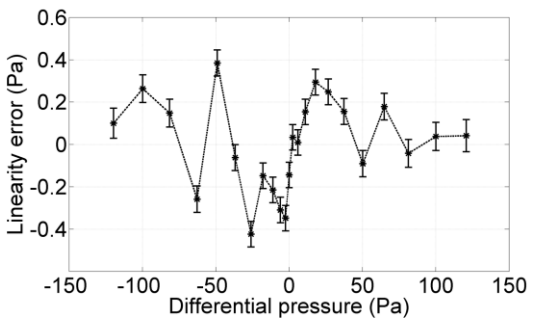

Figure 10. Linearity error of the sensor.

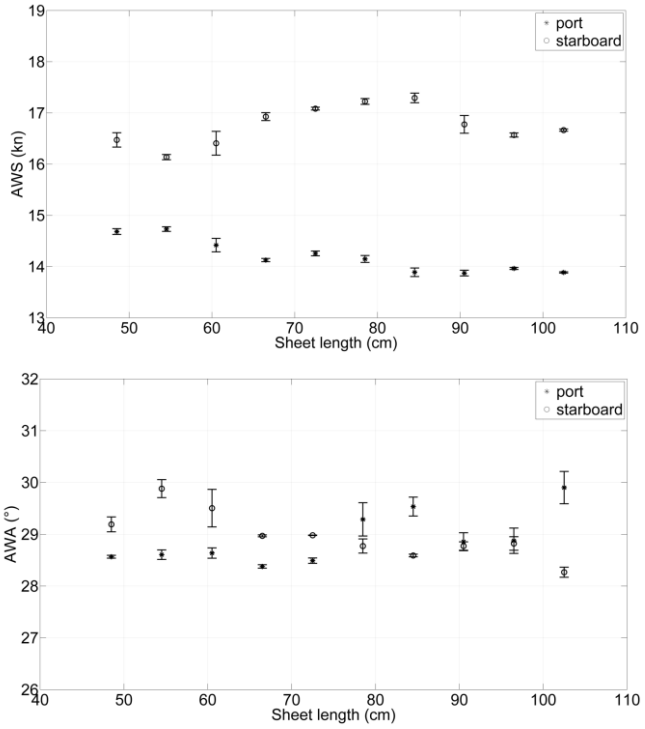

Figure 11. Average Apparent Wind Speed (AWS) during the tests (top) and Average Apparent Wind Angle (AWA) during the tests (bottom).

and AWA). Differential pressure data acquired on both tacks are reported in Figure 13, where the pressure values on the port tack are reversed in sign in order to ease the comparison. On the starboard tack, higher values of differential pressure were measured with a local maximum of about 130 Pa for a sheet length of 65 cm. Loosening the sheet further, determined a not ideal trim of the sail and, consequently, the pressure signal decreased with the result of a reduced boat speed, refer to Figure 12. A similar behaviour can be observed on the pressure data acquired on the port tack but with lower values than those measured on the starboard tack, consistently with a lower AWS as commented above, refer to Figure 11.

With the intent to allow a better comparison of data acquired with different wind speeds (not only between the two tacks but also among data on the same tack), we normalized the pressure signal by the wind dynamic pressure $P_d = \rho AWS^2/2$, yielding

$$\Delta P_{\mathrm{Norm}} = \frac{\Delta P}{P_d}. \tag{6}$$

This because the differential pressure we are considering depends mainly on the shape of the sail, wind incidence angle on

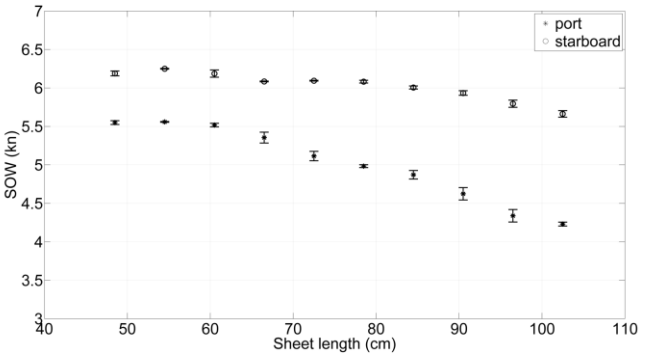

Figure 12. Speed Over Water during the tests.

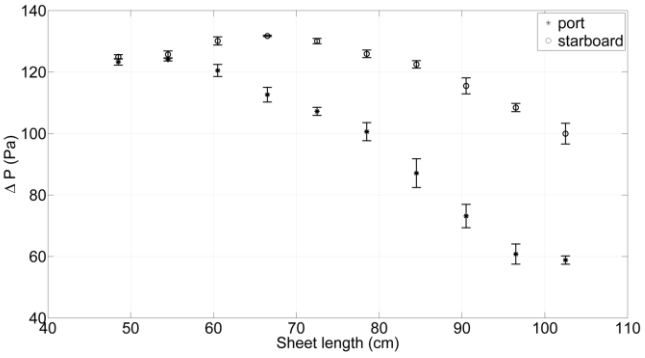

Figure 13. Differential Pressure data on both tacks.

the sail, AWA, that in our case we can assume constant during the whole test campaign (see Figure 11), and wind intensity. The effects of this last dependence can be therefore eliminated by data normalization on the wind dynamic pressure. The normalized pressure data are provided in Figure 14. Again, the behaviour is similar on both tacks, with local maxima measured in conditions of optimal trim of the jib (shorter sheet lengths) where the maxima boat speeds are realized. However, it appears counterintuitive how higher values of normalized pressure difference are recorded on the port tack where, on the contrary, the lowest boat performances are achieved in terms of Speed Over Water.

This unexpected behaviour could be explained by many factors. As a first observation, we have to say that during the navigation the sea conditions were slightly different: at the port side, we sailed with an opposite wave, while in the starboard side we had wave in favour. In particular, taking into account the pitch angle measured during the port and starboard sailing, we observed that the standard deviation of the pitch angle was 1.01 ° and 0.84 °, respectively; this indicates that the wave effect on the boat was about 15 % greater on port side, thus reducing the average boat speed.

As a second observation, the selected position on the sail where the transducer is installed could be not representative of the whole pressure distribution over the entire sail surface on which depends the force developed by sail and therefore the speed of the boat. A further effect can be due to different shape of the sail during the two tacks; this effect is reasonably possible since the boat was equipped with a light jib, that is fit for working in the range of $TWS \in [6, 12]$ kn and we actually were very close to the full-scale range of the sail.

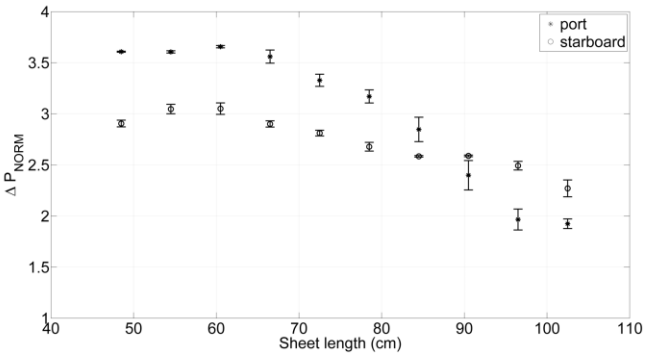

Figure 14. Normalized differential pressure data on both tacks.

4. DISCUSSION AND CONCLUSIONS

The reported results demonstrate that the developed instrument is capable of providing a signal that is uniquely correlated to wind intensity, sail trim, boat course and performance according to Target Data. However, some unexpected results have been obtained which deserved further investigation with additional tests and an improved system. Therefore, future development of this application will have to consider necessarily the adoption of multiple sensors installed and acquired simultaneously, with the aim of obtaining a more accurate description of the pressure distribution over the sail surface. In addition, tests have to be repeated in a larger range of wind conditions, both in terms of apparent wind angle and speed. When this information will be available, it should be possible to obtain a map that links pressure signal to boat performance (speed and course in upwind or downwind conditions).

REFERENCES

[1] Offshore Racing Congress, Velocity Preditcion Program. Online [Accessed 7 November 2023] https://www.orc.org

[2] I. M. Viola, R. G. Flay, Sail aerodynamics: understanding pressure distributions on upwind sails, Experimental Thermal and Fluid Science 35 (2011), pp. 1497-1504. DOI: 10.1016/j.expthermflusci.2011.06.009

[3] F. Fossati, I. Bayati, S. Muggiasca, A. Vandone, G. Campanardi, T. Burch, M. Malandra, Pressure measurements on yacht sails: development of a new system for wind tunnel and full scale testing, Journal of Sailboat Technology 2 (2017), pp. 1-33.

[4] I. Bayati, S. Muggiasca, A. Vandone, Experimental and numerical wind tunnel investigation of the aerodynamics of upwind soft sails, Ocean Engineering 182 (2019), pp. 395-411. DOI: 10.1016/j.oceaneng.2019.04.037

[5] J. Deparday, P. Bot, F. Hauville, B. Augier, M. Rabaud, D. Motta, D. L. Pelley, Modal analysis of pressures on a full-scale spinnaker, Journal of Sailboat Technology 2017-05 (2017), pp. 21.

[6] J. Deparday, P. Bot, F. Hauville, B. Augier, M. Rabaud, D. Motta, D. Le Pelley, Modal analysis of pressures on a full scale spinnaker, The 22nd Chesapeake Sailing Yacht Symposium, Annapolis, USA, 18-19 March 2016. DOI: 10.5957/CSYS-2016-008

[7] J. B. R. G. Souppez, A. Arredondo-Galeana, I. M. Viola, Recent advances in numerical and experimental downwind sail aerodynamics, Journal of Sailing Technology 4 (2019), pp. 45-65. DOI: 10.5957/jst.2019.4.1.45

[8] D. Motta, R. Flay, P. Richards, D. L. Pelley, J. Deparday, P. Bot, Experimental investigation of asymmetric spinnaker aerodynamics using pressure and sail shape measurements, Ocean Engineering 90 (2014), pp. 104–118. DOI: 10.1016/j.oceaneng.2014.07.023

[9] I. Scagnetto, G. Brajnik, P. Gus, F. Trevisan, Oceanus: a context-aware low-cost navigation aid for yacht racing, Journal of Navigation, 74 (2001), pp. 738–749. DOI: 10.1017/S0373463321000205

[10] I. M. Viola, R. G. Flay, Full-scale pressure measurements on a Sparkman and Stephens 24-foot sailing yacht, Journal of Wind Engineering and Industrial Aerodynamics 98 (2010), pp. 800– 807. DOI: 10.1016/j.jweia.2010.07.004

[11] R. G. Flay, Experimental considerations concerning pressure measurements on sails: wind tunnel and full-scale, Proceedings of the International Conference on High Performance Yacht Design, Auckland, NZ, RINA, 14-16 February 2006, pp. 123-130.

[12] W. Graves, T. Barbera, J. Braun, L. Imas, Measurement and simulation of pressure distribution on full size sails, 3rd High Performance Yacht Design Conference, HPYD 2008, Auckland, New Zealand, 1-4 December 2008, pp. 239–246.

[13] A. Gentry, The aerodynamics of sail interaction, Proceedings of the third AIAA Symposium on the Aero/Hydronautics of Sailing, Redondo Beach, USA, 20 November 1971.

[14] Sensirion AG, SDP800-125Pa product page. Online [Accessed 7 November 2023] https://sensirion.com/products/catalog/SDP800-125Pa

[15] Joint Committee for Guide in Metrology, JCGM 100:2008 evaluation of measurement data - guide to the expression of uncertainty in measurement (2008). Online [Accessed 7 November 2023] https://www.bipm.org/documents/20126/2071204/JCGM_100_2008_E.pdf/cb0ef43f-baa5-11cf-3f85-4dcd86f77bd6